**SUPPLEMENTAL FIGURE**

# Kv3.3 channels harboring a mutation of spinocerebellar ataxia type 13 alter excitability and induce cell death in cultured cerebellar Purkinje cells

Tomohiko Irie, Yasunori Matsuzaki, Yuko Sekino, and Hirokazu Hirai

## Supplemental Fig. S1


**Supplemental Figure S1. Amino acid sequence alignment of hKv3.3 (accession number AF022150) with the mKv3.3 used in this experiment**

The two sequences were aligned using Clone Manager 6 software (Scientific & Educational Software, Cary, NC). Hyphens represent gaps introduced to optimize the alignment. The six transmembrane domains are surrounded by squares. Residues conserved between hKv3.3 and mKv3.3 are colored blue.

# Supplemental Fig. S2

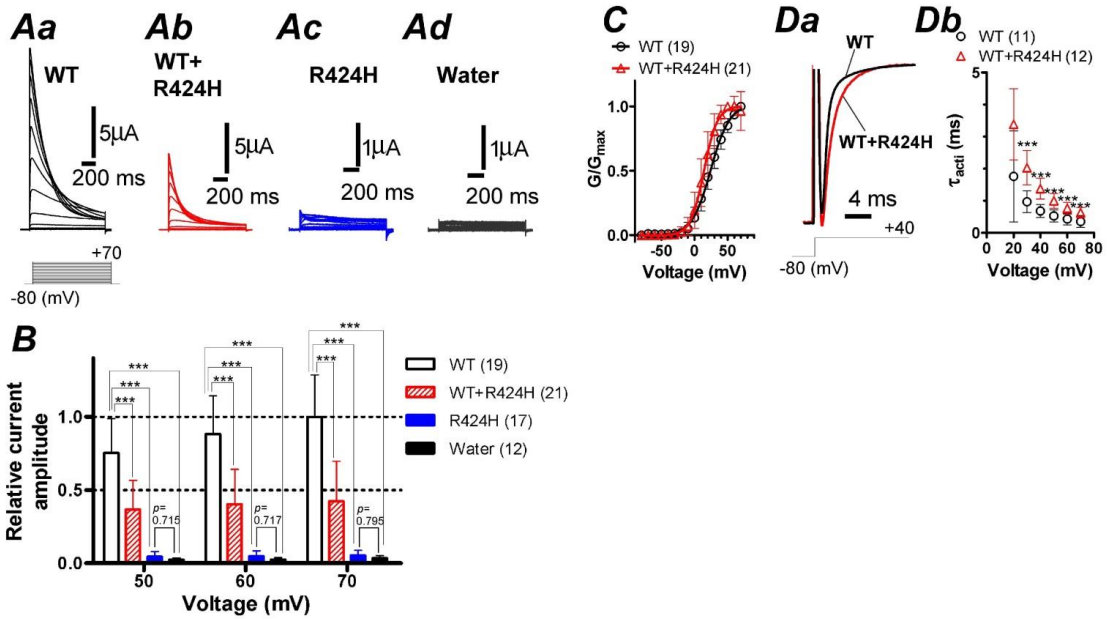


**Supplemental Figure S2. R424H mutant subunits work as a dominant-negative on WT mKv3.3 channels expressed in *Xenopus* oocytes**

*A*, Representative traces evoked by stepping from −80 mV holding potential to voltages ranging from −70 to +70 mV in 10-mV increments. cRNA of WT mKv3.3 (*Aa*, WT), a mixture of WT and R424H mutant subunits at 1:1 ratio (*Ab*, WT+R424H), R424H mutant subunits (*Ac*, R424H), or nuclease-free water (*Ad*, Water) was injected into *Xenopus* oocytes. *B*, Summary of the mean relative current amplitude. The amplitude was calculated from peak amplitude normalized by mean peak amplitude of WT-expressing oocytes at +70 mV voltage pulse. *C*, Normalized conductance (*G*) of WT-expressing and WT+R424H-expressing oocytes are plotted as a function of voltage. *G* was obtained by dividing peak current by electrochemical driving force: $[G = I_K/(V - E_K)]$. The activation ($G/G_{max}$) curves were fit with the Boltzmann function, $G/G_{max} = 1/ [1 + \exp (V_{1/2} - V)/k]$. *D*, Comparison of activation τ between WT-expressing and WT+R424H mutant-expressing oocytes. *Da*, Representative traces evoked by stepping from –80 mV holding potential to +40 mV. The current traces are scaled to the same peak amplitude to compare the activation kinetics. *Db*, Comparison of $\tau_{acti}$ of WT mKv3.3 with that of WT+R424H mutant channels in *Xenopus* oocytes. $\tau_{acti}$ was obtained by fitting current traces with a single exponential function on the rising phases of the traces.

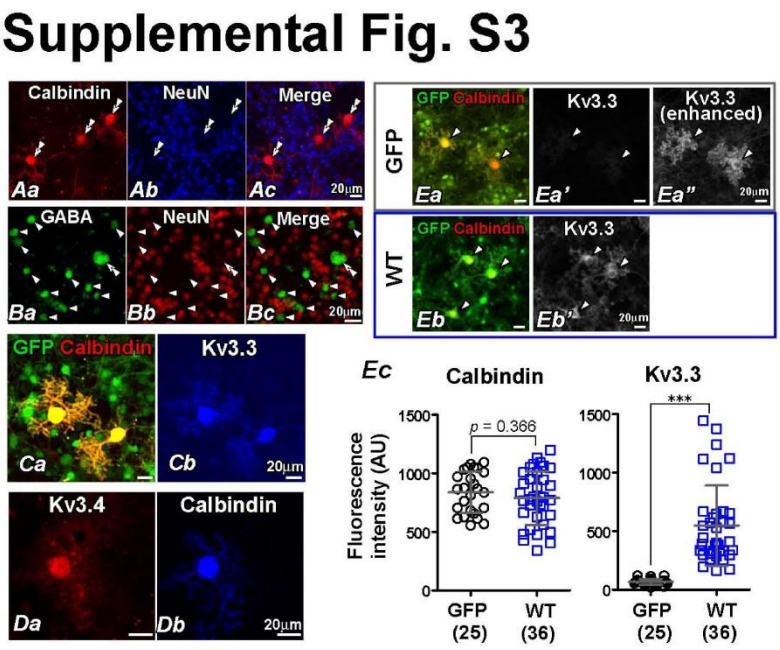


**Supplemental Figure S3. Immunohistochemical characterization of mouse cerebellar cultures**

*A*, Cerebellar cultures double-immunostained with anti-Calbindin and anti-NeuN antibodies at DIV 14. PCs (Calbindin-positive cells in *Aa*, double arrowheads) were NeuN-negative (*Ab* and *Ac*). *B*, Cultures double-immunostained with anti-GABA and anti-NeuN antibodies at DIV 16. GABAergic interneurons (GABA-positive small cells in *Ba* and *Bc*, arrowheads) were also NeuN-negative. Double arrowheads in *Ba* and *Bc* indicate a putative PC. *C*, Cultures triple-immunostained with anti-GFP, anti-Calbindin, and anti-Kv3.3 antibodies at DIV 14. PCs but not other cerebellar neurons expressed mKv3.3 channels. In *C*, GFP-expressing cerebellar cultures were used to visualize the neurons. *D*, Cerebellar cultures double-immunostained with anti-Kv3.4 and anti-Calbindin antibodies, showing the expression of Kv3.4 in PCs. *E*, Immunofluorescence images of cerebellar cultures infected with lentiviral vectors expressing GFP (*Ea*-*Ea"*) or WT subunits (*Eb* and *Eb'*). The cultures were double-immunostained with anti-GFP and anti-Kv3.3 antibodies. The fluorescence images were taken in the same conditions for the quantitative analysis. PCs are indicated by arrowheads. Panel *Ea"* is a contrast-enhanced image of *Ea'* that shows faint but some expression of endogenous mKv3.3 in PCs expressing GFP alone. *Ec*, Quantitative analysis of immunofluorescence intensity for Calbindin and Kv3.3. AU, arbitrary unit. In *A*-*E*, The following primary and secondary antibodies were used. Primary antibodies: mouse monoclonal anti-Calbindin antibody (*A*, *C*, and *D*, 1:2,000-diluted, No.300, Swant; Bellinzona, Switzerland), mouse monoclonal anti-NeuN antibody (*A* and *B*, 1:2,000-diluted), and rabbit polyclonal anti-GABA antibody (*B*, 1:1,000-diluted, A2052; Sigma-Aldrich), guinea pig polyclonal anti-GFP antibody (*C* and *E*, 1:1,000-diluted), and rabbit polyclonal anti-Kv3.3 antibody [*C* and *E*, 1:2,000-diluted, APC-102; Alomone labs, Jerusalem, Israel; This antibody is raised from the peptide KSPITPGSRGRYSRDRAC corresponding with residues 701-718 of rat Kv3.3a channels, which have a sequence that is identical to 692-709 of the mKv3.3 channels (Chang *et al.*, 2007)]. Secondary antibodies: AF 568-conjugated goat anti-rabbit IgG antibody (3*A*), AF 680-conjugated goat anti-mouse IgG antibody (*A* and *D*), AF 488-conjugated goat anti-rabbit IgG antibody (*B*, A-11008; Invitrogen), AF 568-conjugated goat anti-mouse IgG antibody (*B*, *C* , and *E*, A-11031; Invitrogen), AF 488-conjugated goat anti-guinea pig IgG antibody (*C* and *E*), AF 680-conjugated goat anti-rabbit IgG antibody (*C* and *E*, A-21109; Invitrogen). All secondary antibodies were used at the concentration of 5 μg/ml. The incubation conditions were same as Fig. 2. For immunolabeling of Kv3.4 protein in cerebellar cultures (*D*), goat serum was excluded from the incubation buffer. Cerebellar cultures were immunolabeled with goat polyclonal anti-hKv3.4 antibody (1:500-diluted, sc-104343; Santa Cruz Biotechnology, Santa Cruz, CA) and mouse monoclonal anti-Calbindin antibody, and then with AF 568-conjugated donkey anti-goat IgG antibody (A-11057; Invitrogen). After blocking with the incubation buffer containing 10% normal goat serum, the cultures were further incubated with AF 680-conjugated goat anti-mouse IgG antibody.

## Supplemental Fig. S4

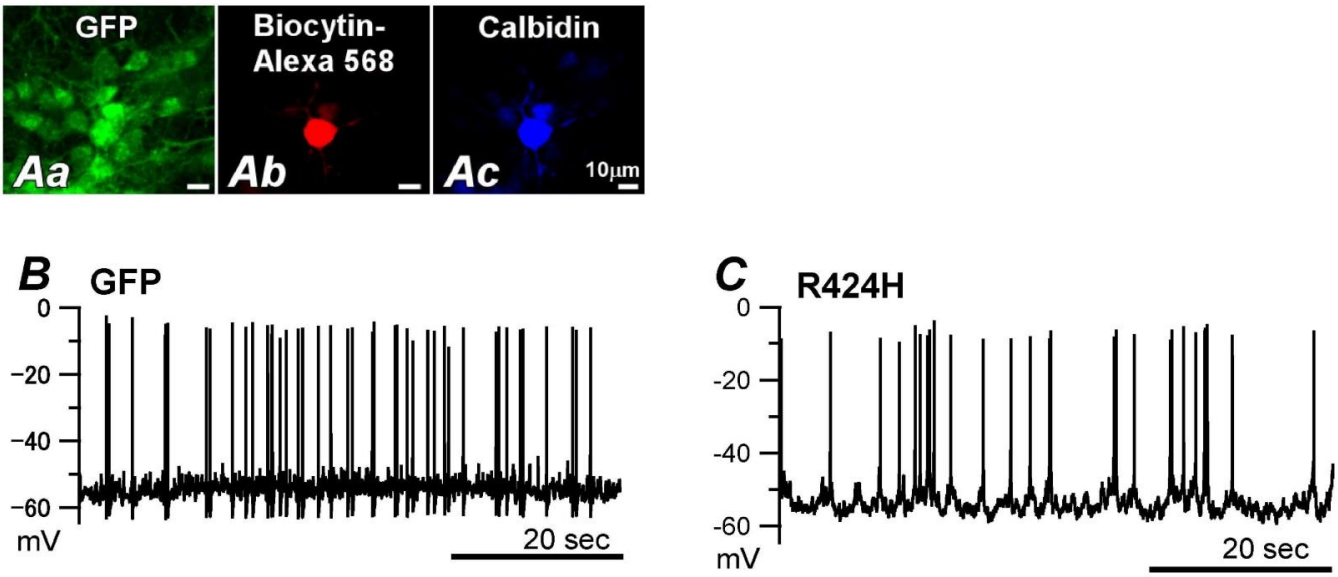


**Supplemental Figure S4. Recordings of spontaneous action potentials from PCs**

*A*, Immunohistochemical identification of PCs. PCs were stained intracellularly with biocytin infused via patch pipettes, fixed in 4% (w/v) formaldehyde, and incubated with mouse monoclonal anti-Calbindin antibody and guinea pig polyclonal anti-GFP antibody. The samples were further incubated with AF 568 streptavidin (S-11226, Invitrogen), AF 488-conjugated goat anti-guinea pig IgG antibody, and AF 680-conjugated goat anti-mouse IgG antibody. The incubation conditions were the same as in Fig. 2. *B* and *C*, Representative spontaneous firing recorded from GFP-expressing PC (*B*) and R424H mutant-expressing PC (*C*) at DIV 8.

## Supplemental Fig. S5

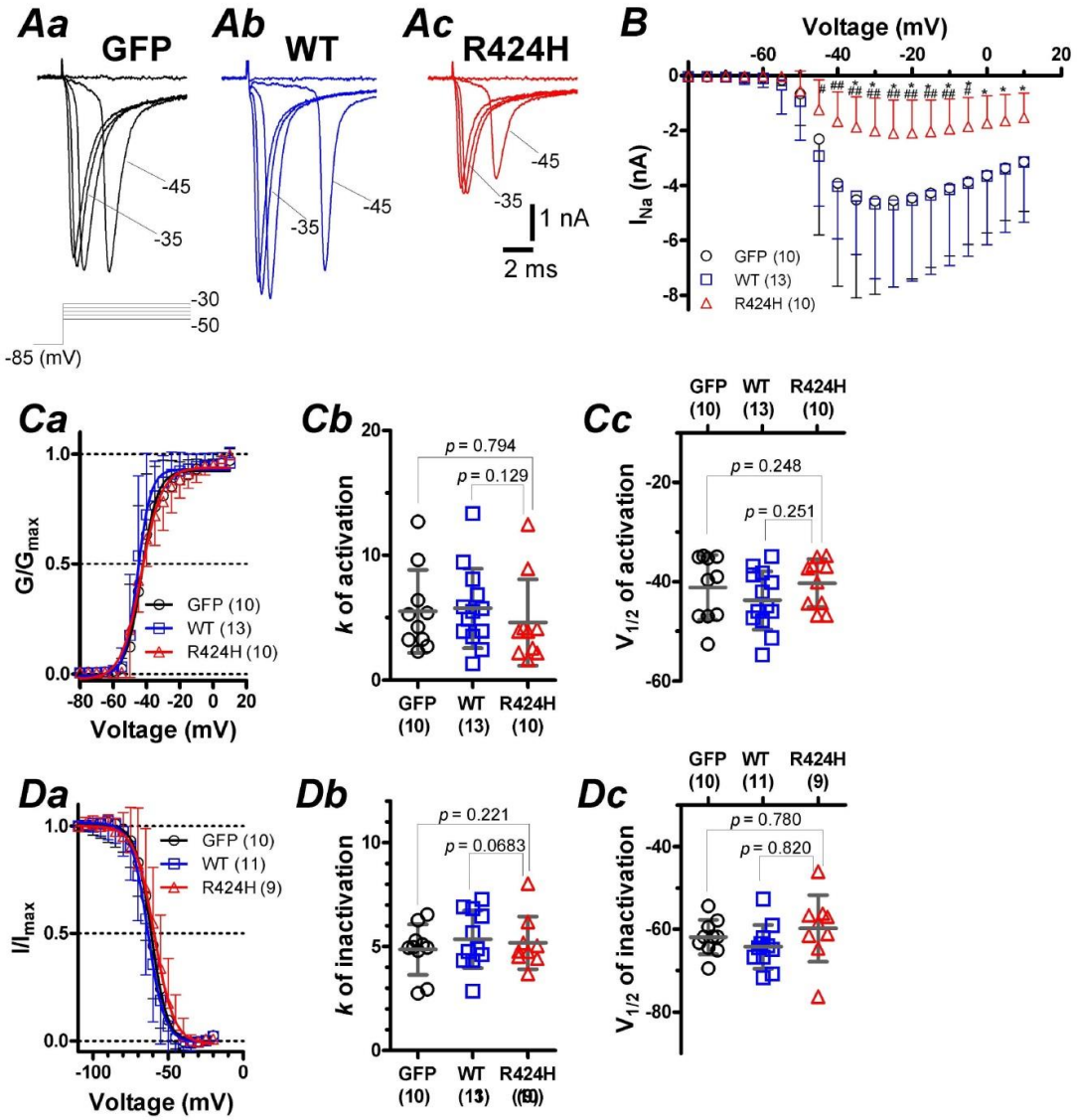


**Supplemental Figure S5. Comparison of $I_{Na}$ recorded under the whole-cell configuration**

$I_{Na}$ was recorded in HEPES-buffered ACSF in which 140 NaCl (in mM) was replaced with 117 NaCl, 22 TEA-Cl, 3 CsCl, and 2 4-aminopyridine, 0.2 $CdCl_2$, 0.1 picrotoxin, and 0.02 DNQX; RT (20-22°C). A CsCl-based internal solution was used (in mM): 140 CsCl, 10 NaCl, 0.2 EGTA, 10 biocytin, and 10 HEPES (pH 7.3 with CsOH, $E_{Na}$ = 63.4 mV). The liquid junction potential (–5 mV) was corrected off-line. *A*, Representative traces of $I_{Na}$ activated with 50-ms voltage steps from –85 mV to voltages ranging from –50 to –30 mV in 5-mV increments. The leak currents were subtracted on-line the p/4 protocol and the $I_{Na}$ was confirmed by application of TTX (0.001 mM, data not shown). *B*, The current-voltage relation of peak $I_{Na}$. In this figure, an asterisk (*) indicates statistical significance between GFP alone and R424H mutant, and a number sign (#) between WT mKv3.3 and R424H. *$p$ < 0.05, #$p$ < 0.05, and ##$p$ < 0.01. *Ca*, The conductance-voltage relations, which were obtained in the same way as those in Supplemental Fig. S2*C*. $E_{Na}$ was used for the equilibrium potential. *Cb* and *Cc*, *k* (*Cb*) and $V_{1/2}$ (*Cc*) of activation for R424H mutant-expressing PCs did not show significant difference compared to those for the control group. *D*, The steady-state inactivation was determined by holding cells at –85 mV before applying a 200-ms pre-pulse to potentials between –125 and –20 mV in 5-mV increments, followed by a 100-ms test pulse to –20 mV. *Da*, Steady-state inactivation curves were obtained in the same way as those in Fig. 1*Bc*. *Db* and *Dc*, *k* (*Db*) and $V_{1/2}$ (*Dc*) for R424H mutant-expressing PCs did not show significant difference compared to those for the control group.